Cusp Points in the Parameter Space of Degenerate 3-RPR Planar Parallel Manipulators

Montserrat Manubens
Institut de Robòtica i Informàtica Industrial,
CSIC - UPC,
Llorens i Artigas, 4-6,
08028 Barcelona, Spain
mmanuben@iri.upc.edu

Guillaume Moroz
INRIA Nancy-Grand Est,
615, rue du jardin botanique,
54600, Villers-lès-Nancy, France
guillaume.moroz@inria.fr

Damien Chablat
Institut de Recherche en Communications
et Cybernétique de Nantes,
UMR CNRS n 6597,
1 rue de la Noë,
44321 Nantes, France
damien.chablat@irccyn.ec-nantes.fr

Philippe Wenger
Institut de Recherche en Communications
et Cybernétique de Nantes,
UMR CNRS n 6597,
1 rue de la Noë,
44321 Nantes, France
philippe.wenger@irccyn.ec-nantes.fr

Fabrice Rouillier
INRIA Paris-Rocquencourt,
Université Pierre et Marie Curie Paris VI
4, place Jussieu,
F-75005 Paris, France
fabrice.rouillier@inria.fr

This paper investigates the conditions in the design parameter space for the existence and distribution of the cusp locus for planar parallel manipulators. Cusp points make possible non-singular assembly-mode changing motion, which increases the maximum singularity-free workspace. An accurate algorithm for the determination is proposed amending some imprecisions done by previous existing algorithms. This is combined with methods of Cylindric Algebraic Decomposition, Gröbner bases and Discriminant Varieties in order to partition the parameter space into cells with constant number of cusp points. These algorithms will allow us to classify a family of degenerate 3-RPR manipulators.

Keywords: kinematics, parallel manipulator, singularities, cusp, discriminant variety, cylindric algebraic decomposition, degenerate 3-RPR, symbolic computation.

1 Introduction

In the past, singularities were believed to physically separate the different assembly modes, meaning that for fixed joint values one could not find a path going from one assembly mode to another without crossing a singular configuration. So the interest relied on considering the widest connected non-singular domain, called *aspect*. Innocenti and Parenti-Castelli pointed out in [1] that non-singular changes of assembly mode are possible, and McAree and Daniel showed in [2] that such changes are possible when triple roots of the Forward Kinematic Problem (FKP) exist. In [3] Zein, Wenger and Chablat showed that for the case of 3-RPR manipulators a non-singular change of assembly mode can be accomplished by encircling a cusp point, and Husty recently proved in [4] that the generic 3-RPR parallel manipulators without joint limits always have 2 aspects.

From the algebraic point of view, the locus of cusp points can be described by means of symbolic equations. In order to avoid long symbolic-algebraic manipulations, these equations are usually solved by numerical approximation at an early stage, which may lead to small deviations that can be propagated along the process. However, there exist efficient symbolic-algebraic techniques that may leave the use of numerical methods to the last step. In particular, we will apply *Gröbner bases* [5] in order to adopt a more suitable equivalent system defining the same solution points.

Lazard and Rouillier introduced the mathematical notion of *Discriminant Variety* (DV) [6], which is a variety of codimension 1 in the chosen parameter space whose com-

plement satisfies the property that over each connected component the given system has a constant number of solutions. The complement of this DV will be partitioned into cells by a *Cylindric Algebraic Decomposition* [7], also known as CAD.

This paper is intended to illustrate both the performance of the new algorithm for the determination of the locus of cusp points and its combination with the forementioned algebraic techniques in the analysis of existence conditions and distribution along a 2-dimensional parameter space. Although the method can be applied to more general manipulators (see [8]), such performance will be exemplified on a family of degenerate 3-RPR manipulators, detailed in Section 2. The algorithm for the cusp point determination, which is one of the main contributions of the paper, is given in Section 3, where it is compared to other previous algorithms. Section 4 outlines some of the exploited algebraic objects such as the DV. In Section 5 the previous procedures are combined with the CAD to partition a 2-dimensional space with regard to the associated number of cusp points, which leads us to analyze a complete family of degenerate 3-RPR manipulators that depend on one geometric parameter. This section also illustrates some applications of the presented strategy to robot design. The paper concludes in Section 6.

2 A class of degenerate 3-RPR

Let us describe the family of manipulators on which the strategies presented along the paper will be exemplified. A general 3-RPR manipulator is a 3-degrees-of-freedom planar parallel mechanism that has two platforms connected by three RPR rods, with the prismatic joints being actuated and the revolute ones being passive. Without loss of generality we can assume the absolute reference frame to be such that the base points of the leg rods are $A_1 = (0,0)$, $A_2 = (A_{2x},0)$ with $A_{2x} > 0$, and $A_3 = (A_{3x},A_{3y})$. If B_1, B_2 and B_3 are the corresponding points on the moving platform, then the geometric parameters associated to this manipulator are the values A_{2x}, A_{3x}, A_{3y}, the lengths $d_1 = \|\overline{B_1B_2}\|$, $d_3 = \|\overline{B_1B_3}\|$, and the angle $\beta = \widehat{B_2B_1B_3}$. The input-space is then formed by $\boldsymbol{\rho} = (\rho_1,\rho_2,\rho_3) \in \mathbb{R}^3$, where $\rho_i \geq 0$ are the leg rod lengths, and the output-space is formed by the poses of the moving platform $\mathbf{x} = (x,y,\alpha)$, where $B_1 = (x,y)$ and α is the angle of vector $B_2 - B_1$ relative to $A_2 - A_1$. We define (s_α, c_α), (s_β, c_β) and $(s_{\alpha+\beta}, c_{\alpha+\beta})$ to denote the sines and cosines of α, β, and $(\alpha+\beta)$, respectively. Then the forward kinematics of a general 3-RPR manipulator is defined by the system of equations

$$\begin{aligned} x^2 + y^2 - \rho_1^2 &= 0 \\ (x + d_1 c_\alpha - A_{2x})^2 + (y + d_1 s_\alpha)^2 - \rho_2^2 &= 0 \\ (x + d_3 c_{\alpha+\beta} - A_{3x})^2 + (y + d_3 s_{\alpha+\beta} - A_{3y})^2 - \rho_3^2 &= 0. \end{aligned} \quad (1)$$

For these manipulators, Hunt showed that the FKP admits at most 6 assembly modes [9], and several authors [10, 11] proved independently that the system associated to the FKP can be reduced to a polynomial of degree 6. The 3-RPR manipulators for which the degree of this characteristic polynomial decreases are known as *analytic* or *degenerate* [12,13], because the Cramer system in Gosselin's method degenerates. In this paper we will focus on a class of degenerate 3-RPR manipulators whose base and moving platforms are congruent triangles, with the moving triangle being reflected with respect to the base one, as that of Fig. 1. This class of manipulators was first studied by Wenger, Chablat and Zein in [14]. Their mathematical description requires the addition to the initial Eqn. (1) of the following geometric constraints:

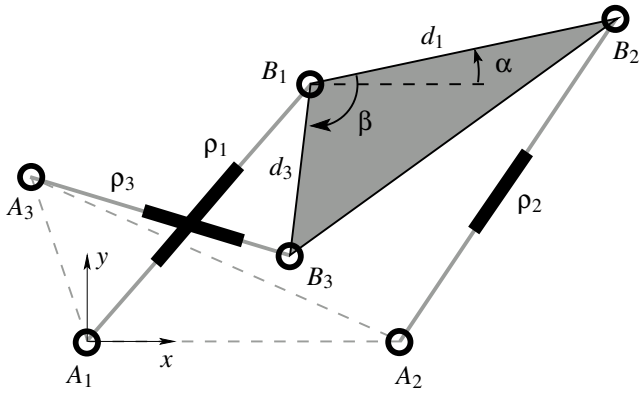

Fig. 1. Example of degenerate 3-RPR.

$$\begin{aligned} d_1 &= A_{2x} \\ \cos(\beta) &= A_{3x}/d_3 \\ \sin(\beta) &= -A_{3y}/d_3. \end{aligned} \quad (2)$$

Therefore, the system of equations defining this family of degenerate 3-RPR manipulators, formed by Eqns. (1) and (2), will be denoted as

$$F(\boldsymbol{\rho}, \mathbf{x}) = 0.$$

Generically, we will refer to this system by F. Whenever concrete values for the geometric parameters are considered, these will be specified. Finally, the notation $|_{(\boldsymbol{\rho},\mathbf{x})}$ will stand for the evaluation on real values $(\boldsymbol{\rho}, \mathbf{x})$.

3 Cusp locus determination

In this section we describe the cuspidal locus and analyze the usual methods for their determination. After that we propose a more accurate approach and compare it to the previous ones in a simple example.

Let us assume that a specific manipulator, whose geometric parameters have been set into F, has been designated. Then, we denote the associated *configuration space* by

$$\mathcal{C}(F) = \{(\boldsymbol{\rho}, \mathbf{x}) \in \mathbb{R}^6 : F|_{(\boldsymbol{\rho},\mathbf{x})} = 0\}.$$

The Jacobian matrix of F with respect to the output variables is denoted as $\mathbf{J}_\mathbf{x}(F) = \left(\frac{\partial F}{\partial x} \; \frac{\partial F}{\partial y} \; \frac{\partial F}{\partial \alpha} \right)$. The configura-

tions where its determinant is zero are called *parallel singular configurations*, or *type 2 singularities*. On these configurations the manipulator shows a loss of control. The *parallel singular locus* of our manipulator is a 2-dimensional space that can be described (see [15]) as

$$\Sigma(F) = \{(\boldsymbol{\rho}, \mathbf{x}) \in \mathcal{C}(F) : \mathbf{J}_{\mathbf{x}}(F)|_{(\boldsymbol{\rho},\mathbf{x})} \text{ is rank deficient}\}.$$

For simplicity, we will refer to this set as the *singular locus*. With this setting we now define the *cuspidal locus* as

$$\kappa(F) = \{(\boldsymbol{\rho}, \mathbf{x}) \in \mathcal{C}(F) : \boldsymbol{\rho} \text{ root of exact multiplicity 3 of } F\},$$

i.e. the triple roots of the FKP. Observe that $\kappa(F) \subset \Sigma(F)$, since the Jacobian $\mathbf{J}_{\mathbf{x}}(F)$ is rank deficient on the roots of multiplicity three of F. It is known that in the proximity of cusp points a non-singular change of assembly mode can be made. Figure 2 shows a cusp point κ and a non-singular path connecting two different assembly modes (p_1 and p_3). We shall note, however, that both the singular and the cusp locus are quite difficult to visualize in the 6-dimensional $(\boldsymbol{\rho}, \mathbf{x})$-space. So for mechanisms with at most one inverse kinematics solution, as is the case for the 3-RPR, we will actually project them onto the input-space instead.

3.1 Usual methods for the cusp computation

Let us revise the two main algorithms that have been more commonly used in the determination of the locus of cusp points for a given manipulator. The following method, introduced by Wenger and Chablat in [13], and anallytically derived in [16], has been used for the degenerate 3-RPR manipulators. It was inspired on an approach developed by Hernández et al in [17] for other robots.

Algorithm 1 by Wenger and Chablat [13]

1. Reduce F (by successive resultants) to a single equation $g(t) = 0$, with $t = \tan(\alpha/2)$ and coefficients in $\boldsymbol{\rho}$.
2. Equations of triple roots of g
   $G = \{g = 0, \frac{\partial g}{\partial t} = 0, \frac{\partial^2 g}{\partial t^2} = 0\}$.
3. Equations of strictly triple roots of g
   $G = G \cup \{\frac{\partial^3 g}{\partial t^3} \neq 0\}$.
4. $\widetilde{G} =$ Eliminate t from G and solve the remaining system for real values of $\boldsymbol{\rho}$.
5. Solve $\widetilde{G}$.

This strategy reduces the problem to the computation of the strictly triple roots of one single univariate polynomial g. However, the constraint added in step 3 makes the computation quite hard, and thus this step is often removed.

Another commonly used method, described by McAree and Daniel in [2], makes use of the series expansion of F.

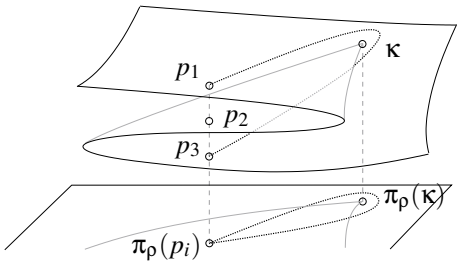

Fig. 2. Cusp point κ as a triple root of the FKP and non-singular path linking upper and lower solutions of the FKP.

Algorithm 2 by McAree and Daniel [2]

1. Series expansion of F
   $\Delta F = \frac{\partial F}{\partial \mathbf{x}}\Delta\mathbf{x} + \frac{\partial F}{\partial \boldsymbol{\rho}}\Delta\boldsymbol{\rho} + \frac{1}{2}\Delta\mathbf{x}^T\left(\frac{\partial^2 F}{\partial \mathbf{x}^2}\right)\Delta\mathbf{x} + \Delta\mathbf{x}^T\left(\frac{\partial^2 F}{\partial \mathbf{x}\partial\boldsymbol{\rho}}\right)\Delta\boldsymbol{\rho} + \frac{1}{2}\Delta\boldsymbol{\rho}^T\left(\frac{\partial^2 F}{\partial \boldsymbol{\rho}^2}\right)\Delta\boldsymbol{\rho} + \ldots$
2. Compute configurations where 1st and 2nd order constraints are rank deficient, i.e. solve
   $\mathbf{v}^T\left(\mathbf{u}\frac{\partial^2 F}{\partial \mathbf{x}^2}\right)\mathbf{v} = 0$, where $\mathbf{v}$ is a unit vector in right kernel of $\frac{\partial F}{\partial \mathbf{x}}$, and $\mathbf{u}$ is a unit vector that spans left kernel.

This second strategy reduces the problem to the resolution of some quadratic equations, but it also requires to find the unit vectors $\mathbf{u}$ and $\mathbf{v}$, which may hinder the computation.

These algorithms are commonly used in the cusp locus determination. However, both have drawbacks related to the non-cuspidality of some resulting points:

- Since the polynomial g obtained by Algorithm 1 is the result of several projections, some of the obtained points may correspond to the projection of complex (not real) solutions, as we will see later on.
- Step 3 usually needs to be removed from Algorithm 1 in order to avoid slow-processing.
- Algorithm 2 does not constrain the multiplicity of the solutions to be exactly 3, so it may obtain higher multiplicity ones. Regardless of that, in [3] it is shown that additional spurious solutions may be produced for generic 3-RPR manipulators.

Therefore, both methods can only provide sufficient conditions for the cuspidal locus but not always necessary ones.

3.2 Improved method

Despite the fact that the formulation of the cusp locus is quite simple, the associated system of equations usually contains many equations in many unknowns, whose resolution can take long computations and even lead to abnormal termination for not too complex examples. So the methods described previously were introduced as simple, though not accurate, alternatives to the symbolic resolution. However, we can now get over some of these difficulties with current powerful symbolic algebra tools that fix the deficiencies of the algorithms detailed above.

The approach that we propose is an evolution of [18] by Moroz et al., inspired on the results of [19]. The main difference of the proposed method compared to that of [18] is the introduction of the *saturation* operator to remove the quadruple roots.

Algorithm 3 Proposed method

1. Equations of double roots of F w.r.t. $\boldsymbol{\rho}$
   $D_F = F \cup \{\det(\mathbf{J}_{\mathbf{x}}(F)) = 0\}$
2. Equations of triple roots of F w.r.t. $\boldsymbol{\rho}$
   $T_F = D_F \cup \{\det(\mathbf{m}) : \mathbf{m} \text{ maximal minors of } \mathbf{J}_{\mathbf{x}}(D_F)\}$
3. Equations of quadruple roots of F w.r.t. $\boldsymbol{\rho}$
   $Q_F = T_F \cup \{\det(\mathbf{m}) : \mathbf{m} \text{ maximal minors of } \mathbf{J}_{\mathbf{x}}(T_F)\}$
4. Saturate T_F by Q_F
   $C_F = \text{sat}(T_F, Q_F)$
5. Solve C_F for real values of $(\boldsymbol{\rho}, \mathbf{x})$

Given the system defining the mechanism F, it computes iteratively the equations T_F and Q_F of triple and quadruple roots $\boldsymbol{\rho}$ of F, respectively. Then, we use saturation. Given two polynomial systems S_1 and S_2, $\text{sat}(S_1, S_2)$ is an algebraic operator that returns a polynomial system whose solution set is the closure of the solutions of the first system after removing those of the second one. If $V(S_i)$ denotes the solution set of S_i, it is satisfied that

$$\overline{V(\text{sat}(S_1, S_2))} = \overline{V(S_1) \setminus V(S_2)}. \tag{3}$$

In general, the saturation ensures that all roots of S_2 are removed. However, in specific cases, some points can remain due to property of Eqn. (3) for which we can only obtain $\overline{V(S_1) \setminus V(S_2)}$ instead of $V(S_1) \setminus V(S_2)$, which can differ by a null-measure set that can easily be removed afterwards. Further details on the saturation and its geometric interpretation can be found in [5].

Although we are only interested in real (feasible) solutions, we shall note that the polynomial system obtained after saturating has real coefficients and thus its solution set could contain some complex (not real) roots. For this reason we need to solve the final cusp system C_F in the real field. This is done by using the *RootFinding* Maple package.

With Algorithm 3 the previous drawbacks are amended:

- When computing the saturation of T_F by Q_F, the points of multiplicity 4 or higher are removed, and so we can guarantee that only the cusp locus is obtained.
- By solving C_F for $(\boldsymbol{\rho}, \mathbf{x})$, instead projecting onto the $\boldsymbol{\rho}$-space, we avoid having biased points produced by the projection of complex (not real) solutions.
- Furthermore, solving C_F in the real field ensures that no other spurious complex solutions are considered.

3.3 Case study comparison

Let us now compare the performance of both Algorithm 1 without step 3 and the proposed Algorithm 3 on a simple case of degenerate 3-RPR in order to contrast their results. However, let us clarify that both the formulation and the proposed algorithm apply to other more general manipulators (see [8]). We set the geometric parameter values $A_{2x} = 1$, $A_{3x} = 0$, $A_{3y} = 1$, $\beta = -\pi/2$, $d_1 = 1$, and $d_3 = 1$.

The characteristic polynomial for Algorithm 1 is

$$g(t) = (\rho_3^2 - \rho_1^2)t^3 + (\rho_2^2 - \rho_1^2 - 4)t^2 + (\rho_3^2 - \rho_1^2 - 4)t + \rho_2^2 - \rho_1^2$$

After eliminating t from G we get $\widetilde{G} = \{P_1, P_2, P_3\}$ as follows

$$\begin{aligned} \rho_2^4 + \rho_3^4 - 2\rho_2^2\rho_3^2 + 6\rho_1^2 - 3\rho_2^2 - 3\rho_3^2 - 12 &= 0 \\ 2\rho_1^4 + 2\rho_3^4 - 4\rho_1^2\rho_3^2 + 4\rho_1^2 + 3\rho_2^2 - 7\rho_3^2 - 16 &= 0 \\ \rho_3^4 + \rho_1^2\rho_2^2 - \rho_1^2\rho_3^2 - \rho_2^2\rho_3^2 + 3\rho_1^2 + \rho_2^2 - 4\rho_3^2 - 6 &= 0. \end{aligned} \tag{4}$$

Observe that these equations are not independent. Indeed, P_2 is a combination of the other two:

$$P_2 = \frac{(\rho_1^2 - \rho_3^2 + 1)}{3} P_1 + \frac{(\rho_3^2 - \rho_2^2 + 6)}{3} P_3.$$

Additionally, there are solutions of $\widetilde{G}$ that do not correspond to the real cusp locus. For instance, if we set $\rho_1 = 1/3$, the system $\widetilde{G}|_{\rho_1 = 1/3}$ has two solutions with both ρ_2 and ρ_3 positive. But the FKP evaluated on these two solutions only has complex solutions (x, y, α). So, for $\rho_1 = 1/3$ the c-space $\mathcal{C}(F)$ has no cusp points, though Algorithm 1 obtained two mistaken candidates.

We now test Algorithm 3 on the same example. The equations of the cusp locus C_F are:

$$\begin{aligned} 6c_\alpha + \rho_2^2 - \rho_3^2 &= 0 \\ 2s_\alpha^2 + s_\alpha - 1 &= 0 \\ 2c_\alpha^2 - s_\alpha - 1 &= 0 \\ 2c_\alpha s_\alpha - c_\alpha &= 0 \\ 3c_\alpha + 3s_\alpha + \rho_1^2 - \rho_3^2 + 1 &= 0 \\ 3c_\alpha + 3s_\alpha + x^2 + y^2 - \rho_3^2 + 1 &= 0 \\ 2xs_\alpha + 2ys_\alpha - 4s_\alpha - x - y + 2 &= 0 \\ 2s_\alpha\rho_3^2 - 3c_\alpha - 6s_\alpha - 4xy - x - y &= 0 \\ 2xc_\alpha + 2ys_\alpha + c_\alpha - 3s_\alpha - 2x + 1 &= 0 \\ 2yc_\alpha + 2ys_\alpha + c_\alpha - s_\alpha - x + y + 1 &= 0 \\ 4ys_\alpha - s_\alpha + 2(c_\alpha - 1)\rho_3^2 + 4y^2 - 3y + x + 1 &= 0 \\ 2s_\alpha(2y^2 - 4y - 1) - 3c_\alpha - 4xy - 2y^2 + 3y & \\ -x + \rho_3^2 - 2 &= 0 \\ 6s_\alpha(2y + 1) + 12c_\alpha - 8y^2x + 8y^3 + 12xy & \\ +x - 3y + 2x\rho_3^2 - 6y\rho_3^2 - 6\rho_3^2 + 8 &= 0 \\ 18s_\alpha(18y - 1) + 36c_\alpha + 32y^4 + 20y^2 + 44xy & \\ +13x - 47y + 4\rho_3^4 - 8\rho_3^2yx - 32y^2\rho_3^2 & \\ -6x\rho_3^2 - 6y\rho_3^2 - 32\rho_3^2 + 40 &= 0. \end{aligned} \tag{5}$$

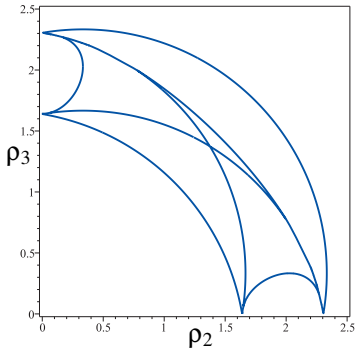

Fig. 3. Singular curve for $\rho_1 = \frac{1}{3}$ on (ρ_2, ρ_3)

Here if we try to solve $C_F|_{\rho_1=1/3}$, we get no real solutions. Figure 3 shows a section in the (ρ_2, ρ_3)-plane of the singular locus of F for $\rho_1 = \frac{1}{3}$. As can be observed, there is no cusp point in this plot. This phenomenon is not casual. Actually, the value $1/3$ for ρ_1 has not been randomly picked as we will see in next section. In fact, Algorithm 3 describes the cusp locus more accurately than Algorithm 1, in general.

4 Discussion on the joint space

We now extend our improved method to partition a parameter space with regard to the associated cusp locus. So, we want to discuss the solutions of a parametric system. Among the numerous possible ways of solving parametric systems, we focus on the use of Discriminant Varieties (DV) [6] for two main reasons: it provides a formal decomposition of the parameter space through an exactly known algebraic variety (no approximation), and it has been successfully used in similar problems [20].

Let us consider a general parametric polynomial system

$$\mathcal{F} = \{p_1(\mathbf{v}) = 0, \ldots, p_m(\mathbf{v}) = 0, q_1(\mathbf{v}) > 0, \ldots, q_l(\mathbf{v}) > 0\},$$

where $p_1, \ldots, p_m, q_1, \ldots, q_l$ are polynomials with rational coefficients depending on $\mathbf{v} = (U_1, \ldots, U_d, X_1, \ldots, X_n)$ with X_i being unknowns and U_i parameters. For instance, the system describing the cuspidal configurations our manipulator C_F is parametric if some of the geometric parameters are initially left free in F. The DV associated to system $\mathcal{F}$ is described by a polynomial equation. This DV partitions the parameter space into several regions such that over each open region delimited by the DV the number of real solutions of $\mathcal{F}$ is constant. Prior to defining the DV associated to $\mathcal{F}$, we need to specify a solver of 0-dimensional systems that will be used as a black box.

4.1 Basic black-boxes

Let us describe the global solver for 0-dimensional systems that will be used as a black box in the general algorithm. We mainly use exact computations, namely formal elimination of variables (resultants, Gröbner bases) and resolution of 0-dimensional systems, including univariate polynomials.

We first compute a Gröbner basis of the ideal $\langle p_1, \ldots, p_m \rangle$ for any ordering, which will help us detect if the system has or has not finitely many complex solutions. If yes, then compute a so called Rational Univariate Representation (RUR) of $\langle p_1, \ldots, p_m \rangle$ (see [21]), which is an equivalent system of the form

$$\{f(T) = 0, X_1 = \tfrac{g_1(T)}{g(T)}, \ldots, X_n = \tfrac{g_n(T)}{g(T)}\},$$

where T is a new variable independent of $X_1, \ldots, X_n$, equipped with a so called *separating element* (injective on the solutions of the system) $u \in \mathbb{Q}[X_1, \ldots, X_n]$ and such that :

$$\begin{array}{ccccc} V(p_1, \ldots, p_m) & \xrightarrow{u} & V(f) & \xrightarrow{u^{-1}} & V(p_1, \ldots, p_m) \\ (x_1, \ldots, x_n) & \mapsto \beta = u(x_1, \ldots, x_n) & & \mapsto & \left(\frac{g_1(\beta)}{g(\beta)}, \ldots, \frac{g_n(\beta)}{g(\beta)}\right) \end{array}$$

defines a bijection between the (real) roots of the system and the (real) roots of the univariate polynomial f.

We then solve $f = 0$, computing so called isolating intervals for its real roots, i.e. non-overlapping intervals with rational bounds that contain a unique real root of f (see [22]). Finally, interval arithmetic is used in order to get isolating boxes of the real roots of the system (non-overlapping products of intervals with rational bounds containing a unique real root of the system), by studying the RUR over the isolating intervals of f.

In practice, we use the function *RootFinding[Isolate]* from Maple software, which performs exactly the computations described above.

4.2 Discriminant varieties

Consider now the constructible set

$$\mathcal{S} = \{\mathbf{v} \in \mathbb{C}^n : p_1(\mathbf{v}) = 0, \ldots, p_m(\mathbf{v}) = 0, \\ q_1(\mathbf{v}) \neq 0, \ldots, q_l(\mathbf{v}) \neq 0\},$$

and let us assume that for almost all the parameter values this $\mathcal{S}$ is a finite set of points. Then, a discriminant variety of $\mathcal{S}$ with respect to $(U_1, \ldots, U_d)$ is a variety $\mathcal{V} \subset \mathbb{C}^d$ such that over each connected open set $\mathcal{U}$ not intersecting $\mathcal{V}$ ($\mathcal{U} \cap \mathcal{V} = \emptyset$), $\mathcal{S}$ defines an analytic covering. In particular, the number of points of $\mathcal{S}$ over any point of $\mathcal{U}$ is constant.

Discriminant varieties can be computed using basic and well-known tools from computer algebra such as Gröbner bases [6]. A full package is available in Maple software through the *RootFinding[Parametric]* package, which provides us with a polynomial $DV(\mathcal{S}; U_1, \ldots, U_d)$ whose associated discriminant variety is $\mathcal{V}$.

4.3 Case study comparison

Let us consider again the degenerate 3-RPR with the same geometric parameter values as those specified in section 3.3, i.e. $A_{2x} = 1$, $A_{3x} = 0$, $A_{3y} = 1$, $\beta = -\pi/2$, $d_1 = 1$, and $d_3 = 1$, and consider the systems $\widetilde{G}$ (Eqn. 4), and C_F (Eqn. 5), obtained by Algorithm 1 without step 3 and by Algorithm 3, respectively. We will regard as a parameter one of the leg lengths ρ_1 of the manipulator. The discriminant

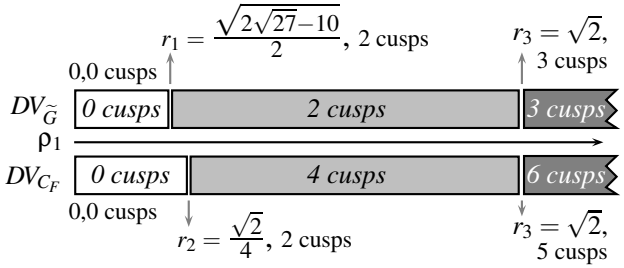

Fig. 4. Comparison of both discussions on ρ_1

variety will provide us with a polynomial in ρ_1 whose roots will delimit some open intervals such that for whatever value of ρ_1 within one interval, the number of cusp points of $F|_{\rho_1}$ will be the same. We compute the DV for each system with respect to ρ_1, and analyze the results.

In the first case, we get the polynomial $DV(\widetilde{G};\rho_1) = \rho_1(\rho_1^2-2)(2\rho_1^4+10\rho_1^2-1)$, whose roots describing the discriminant variety are

$$r_0 = 0, \quad r_1 = \frac{\sqrt{2\sqrt{27}-10}}{2} \quad \text{and} \quad r_3 = \sqrt{2}.$$

Since the number of cusp points is kept constant between two consecutive roots, we can compute the associated number of cusps by picking one single value of ρ_1 inside each open interval and solve $\widetilde{G}|_{\rho_1}$. In this case we obtain

- 0 cusp configurations for $\rho_1 \in]0, r_1[$,
- 2 cusp configurations for $\rho_1 \in]r_1, r_3[$, and
- 3 for $\rho_1 \in]r_3, \infty[$.

Substituting $\rho_1 = r_i$ into $\widetilde{G}$ we obtain the number of cusps on the borders of the intervals.

- 0 cusps on $\rho_1 = 0$,
- 2 cusps on $\rho_1 = r_1$, and
- 3 on $\rho_1 = r_3$.

In the second case, a similar analysis for C_F gives

$$DV(C_F;\rho_1) = \rho_1(\rho_1^2-2)(8\rho_1^2-1)(2\rho_1^4+10\rho_1^2-1),$$

which has one more root than $DV(\widetilde{G};\rho_1)$

$$r_0 = 0, \quad r_1 = \frac{\sqrt{2\sqrt{27}-10}}{2}, \quad r_2 = \frac{\sqrt{2}}{4} \quad \text{and} \quad r_3 = \sqrt{2}.$$

The intervals and the numbers of cusps for C_F differ a bit from those obtained for $\widetilde{G}$:

- 0 cusps for $\rho_1 \in]0, r_1[$,
- 0 cusps for $\rho_1 \in]r_1, r_2[$,
- 4 cusps for $\rho_1 \in]r_2, r_3[$,
- 6 cusps for $\rho_1 \in]r_3, \infty[$.
- 0 cusps on $\rho_1 = 0$,
- 0 cusps on $\rho_1 = r_1$,
- 2 cusps on $\rho_1 = r_2$,
- 5 cusps on $\rho_1 = r_3$.

The results obtained in both cases are compared in Fig. 4. We can observe that the first two intervals do not exactly coincide, and that for the second system the obtained numbers of cusps appear doubled for all intervals (compared to those obtained for the first system). Both phenomena can be explained as a consequence of the projection map used to compute the system $\widetilde{G}$. Let us remind the reader that $\widetilde{G}$ is obtained after several reductions of the initial system, each of which applying also a projection on the $\boldsymbol{\rho}$-space. For this, there can be complex configurations of the manipulator that project onto real roots $\boldsymbol{\rho}$ of $\widetilde{G}$. This is the case for the values of $\rho_1 \in]r_1, r_2[$.

The same can be done for any other parameter and the same phenomena can be observed.

5 Higher-dimensional discussion by means of a CAD

By construction we know that over any connected open region not intersecting the DV the system has a constant number of real roots, for whatever chosen parameters. But if we want to discuss larger parameter spaces, then the open regions will no longer be as simple as 1-dimensional intervals. So the goal of this section is to provide an accurate description of the regions with constant number of solutions. For this we will use the Cylindric Algebraic Decomposition (CAD) [7, 23].

5.1 The complementary of a discriminant variety

Let $\mathcal{P}_d \subset \mathbb{Q}[U_1, \ldots, U_d]$ be the set of polynomials describing the DV. Then for each $i = d-1, \ldots, 0$, we introduce a new set of polynomials $\mathcal{P}_i \subset \mathbb{Q}[U_1, \ldots, U_{d-i}]$ defined by a backward recursion:

- $\mathcal{P}_d$ = the polynomials defining the DV,
- $\mathcal{P}_i = \{\, DV(p; U_i),\ \text{LeadingCoefficient}(p, U_i),$
  $\text{Resultant}(p, q, U_i),\ p, q \in \mathcal{P}_{i+1}\}$

Each $\mathcal{P}_i$ has an associated algebraic variety of dimension at most $i-1$, $\mathcal{V}_i = V(\prod_{p\in\mathcal{P}_i} p)$. The $\mathcal{V}_i$ are used to recursively define a finite union of simply connected open subsets $\cup_{k=1}^{n_i} \mathcal{U}_{i,k} \subset \mathbb{R}^i$ of dimension i such that $V_i \cap \mathcal{U}_{i,k} = \emptyset$.

Before defining the sets $\mathcal{U}_{i,k}$, we introduce some notation: for a univariate polynomial p with n real roots,

$$\text{root}(p, l) = \begin{cases} -\infty \text{ if } l \leq 0, \\ \text{the } l^{th} \text{ real root of } p \text{ if } 1 \leq l \leq n, \\ +\infty \text{ if } l > n\ . \end{cases}$$

Moreover, if p is a n-variate polynomial, and $\mathbf{v}$ is a $(n-1)$-tuple, then $p^{\mathbf{v}}$ denotes the univariate polynomial where the first $n-1$ variables have been replaced by $\mathbf{v}$.

The recursive process defining the $\mathcal{U}_{i,k}$ is the following:

- For $i = 1$, let $p_1 = \prod_{p\in\mathcal{P}_1} p$.
  Taking all $\mathcal{U}_{1,k} =]\text{root}(p_1, k); \text{root}(p_1, k+1)[$ for $k = 0, \ldots, n$, where n is the number of real roots of p_1, one gets a partition of $\mathbb{R}$ that fits the above definition. Moreover, one can arbitrarily chose one rational point $u_{1,k}$ in each open interval $\mathcal{U}_{1,k}$.
- Then, for $i = 2, \ldots, d$, let $p_i = \prod_{p\in\mathcal{P}_i} p$.
  The regions $\mathcal{U}_{i,k}$ and the points $u_{i,k}$ are of the form:

$$\begin{aligned} \mathcal{U}_{i,k} =& \{(v_1, \ldots, v_{i-1}, v_i) \mid \mathbf{v} := (v_1, \ldots, v_{i-1}) \in \mathcal{U}_{i-1,j}, \\ & v_i \in]\text{root}(p_i^{\mathbf{v}}, l), \text{root}(p_i^{\mathbf{v}}, l+1)[\} \\ u_{i,k} =& (\beta_1, \ldots, \beta_{i-1}, \beta_i), \text{ with} \\ & \begin{cases} (\beta_1, \ldots, \beta_{i-1}) = u_{i-1,j} \\ \beta_i \in]\text{root}(p_i^{u_{i-1,j}}, l), \text{root}(p_i^{u_{i-1,j}}, l+1)[\ , \end{cases} \end{aligned}$$

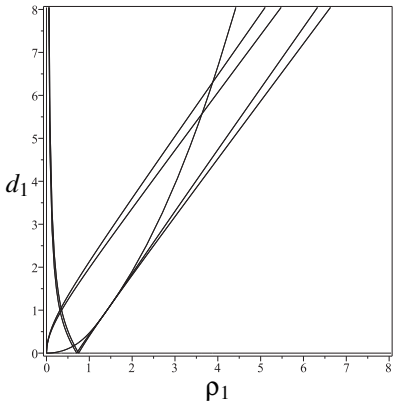

Fig. 5. Plot of the DV of C_F with respect to (ρ_1, d_1)

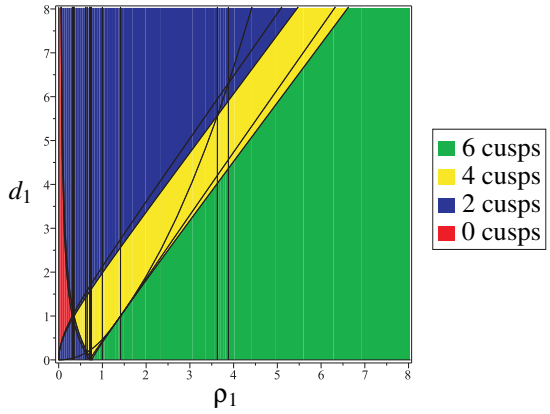

Fig. 6. Cell Decomposition for (ρ_1, d_1)

where j, l are fixed integers.

With this recursive procedure we get a full description of the complementary of the DV for the system to be solved: the cells $\mathcal{U}_{d,k}$ and a test point $u_{d,k} \in \mathcal{U}_{d,k}$ (with rational coordinates). The number of solutions associated to each open cell $\mathcal{U}_{d,k}$ is obtained by solving the given system restricted to $u_{d,k}$ using a 0-dimensional solver. Both the cell decomposition and the test points can be obtained by the Maple function *RootFinding[Parametric][CellDecomposition]*.

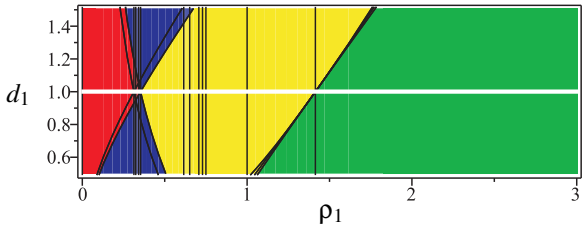

Fig. 7. Zoom in of the cell decomposition for (ρ_1, d_1). Line $d_1 = 1$ in white.

5.2 Open CAD for a class of degenerate 3-RPR

Let us see the performance of this CAD on a 2-dimensional discussion. We consider now a family of degenerate 3-RPR manipulators with $A_{2x} = 1$, $A_{3x} = 0$, $A_{3y} = 1$, $\beta = -\pi/2$, and $d_3 = 1$, and regard as parameters both ρ_1 and d_1, constrained by $d_1 \geq 0$. Now, the system C_F describing the cusp locus associated to this family of manipulators has 18 polynomials, its DV is plot in Fig. 5, and the polynomial $DV(C_F; \rho_1, d_1)$ factors as follows:

$$
\begin{aligned}
& d_1 \rho_1 (d_1^2+1)(-4\rho_1^6 - 12\rho_1^4 + 27\rho_1^2 d_1^2 + 15\rho_1^2 - 4) \\
& (4\rho_1^6 + 12\rho_1^4 d_1^2 - 15\rho_1^2 d_1^4 + 4 d_1^6 - 27\rho_1^2 d_1^2) \\
& (256\rho_1^6 d_1^2 + 81\rho_1^2 d_1^6 - 288\rho_1^4 d_1^4 + 256\rho_1^6 - 576\rho_1^4 d_1^2 \\
& + 51\rho_1^2 d_1^4 - 16 d_1^4 - 288\rho_1^4 + 51\rho_1^2 d_1^2 + 81\rho_1^2).
\end{aligned}
$$

The complement of this DV produces 90 cells with associated numbers of cusps varying among 0, 2, 4 and 6, as shown in Fig. 6, where black vertical lines delimit intersection points of the DV. Let us notice that although all cells must be considered disconnected, it is apparent that cells are naturally grouped with regard to their number of cusps. Additionally, cells with different number of cusps are exclusively separated by curves of the discriminant variety. Furthermore, this distribution is consistent with that obtained for $d_1 = 1$ in Section 4.3, as can be seen in Fig. 7. However, here the section is divided into many more smaller intervals whose borders we cannot apriori ensure to be associated to a specific number of cusp points. In fact, let us also observe that the cells with 2 cusp points (in blue) degenerate into one single point for $d_1 = 1$. So we could claim that the case with $d_1 = 1$ is a very special degenerate 3-RPR manipulator.

5.3 Study of the cusp points on the borders of the CAD

At this point we can only certify the number of cusp points in the open cells. This excludes the cell borders. The union of all these borders consists of the DV plus the delimitation of intersection points of the DV. However, by definition, changes in the number of solutions can only happen on the DV. So, we just need to analyze the DV.

We could try executing a further iteration of the CAD on the DV, but the system to be solved turns out to be too complex and we cannot obtain any results after long computations. It is clear that not all points on the DV will correspond to the same number of solutions. But we can expect the number of solutions to be preserved along the DV between two consecutive auto-intersection points of the DV. And although it has not yet been proven, many tests have been run on several examples with random points on the DV and all the results confirm what the following conjecture infers.

Conjecture 1. Given a polynomial system F, let $\mathcal{V}$ be the DV of F w.r.t two parameters U_1, U_2, and let $\mathcal{A}$ be the set of its auto-intersection points. Then, the number of solutions of F is constant on each connected component of $\mathcal{V} \setminus \mathcal{A}$.

The following algorithm analyzes the to study the numbers of solutions on the DV based on the previous conjecture.

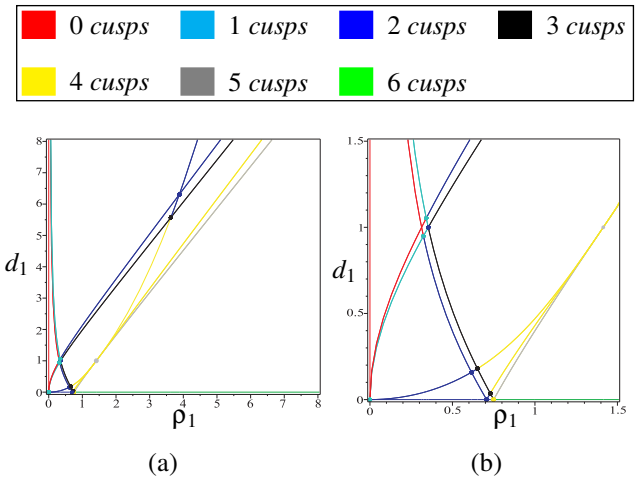

(a) (b)

Fig. 8. Distribution of cusp points on $DV(C_F;\rho_1,d_1)$ (a), and zoom in view on $[0,1.5]\times[0,1.5]$ (b).

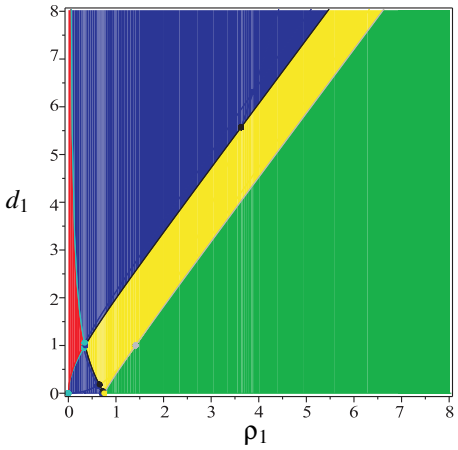

Fig. 9. Complete analysis of the cusp points for (ρ_1,d_1)

Algorithm 4 Number of solutions of F on the DV

$\mathcal{V}=$ variety of $DV(F;U_1,U_2)$
$\mathcal{A}=\{$auto-intsersection points of $\mathcal{V}\}$
for each connected component $\mathcal{U}_i$ of $\mathcal{V}\setminus\mathcal{A}$ **do**
  $p_i=$ random point on $\mathcal{U}_i$
  Compute the number of solutions on $\mathcal{U}_i$ as the number of solutions of $F|_{p_i}$
end for
for each point $q\in\mathcal{A}$ **do**
  Compute the number of solutions of $F|_q$
end for

5.4 Complete analysis and applications

From the results exposed in the previous subsections and by joining all the different pieces together we obtain a complete partition of the 2-dimensional parameter space.

The execution of Algorithm 4 on $DV(C_F;\rho_1,d_1)$ provides the distribution of cusp points shown in Fig. 8. The integral picture of the 2-dimensional distribution is given in Fig. 9. It is interesting to notice that there is a continuity on the transitions between cells having the same number of cusp points, since their common border inherits that same number of cusp points.

Observe also that this distribution has been obtained thanks to the DV associated to the chosen parameters d_1 and ρ_1, which depends exclusively on these two parameters. In particular, $DV(C_F;\rho_1,d_1)$ does not depend on ρ_2 nor ρ_3. This tends to be erroneously interpreted as:
"*if we pick a* (ρ_1,d_1)*-point with associated number of cusps k, then whatever the values* ρ_2 *and* ρ_3 *may take,* $C_F|_{(\rho_1,\rho_2,\rho_3,d_1)}$ *has k solutions*".
Instead, it should be read as follows:
"*if we pick a* (ρ_1,d_1)*-point with associated number of cusps k and fix these values then, among the reachable configurations there are k cuspidal ones, i.e.* $C_F|_{(\rho_1,d_1)}$ *has k solutions*". However, the number of associated cusp points does establish a maximum of cuspidal configurations for any values ρ_2 and ρ_3. For example, in yellow regions we can have a maximum of 4 cuspidal configurations, but depending on the values of ρ_2 or ρ_3 there can even be none. In particular, for the red regions there are 0 cusp points for all possible values ρ_2 and ρ_3.

Some applications can be derived which may be interesting from the designer's point of view:

- It can be helpful in deciding the most suitable architecture of the mechanism. Let us assume that we want to design a 3-RPR manipulator with some given geometric constraints such that for a specific task one of the legs has to be blocked to a fixed length ρ_1, but the job requires a large singularity-free workspace. Therefore, we may be interested in finding a range Δd_1 of parameter values for which the manipulator is cuspidal.
- It can also be useful for deciding the most suitable ranges of leg lenghts for each possible architecture, given a specific task. For instance, let us assume that the job is set for a non-cuspidal manipulator with parameter values $A_{2x}=1, A_{3x}=0, A_{3y}=1, \beta=-\pi/2$, and $d_3=1$, but it requires the largest possible range of the leg length ρ_1. Then, the value d_1 can be optimized with this criterion. Figure 10 details both the optimal valule d_1 and the largest possible range $\Delta\rho_1$ for our problem.

Let us just notice that in both cases the obtained ranges can be of varied topology (open, closed, semi-closed, open and closed, connected, or even a union of these types). This is due to the combination of both the CAD and the study of the cusp locus on the DV.

6 Conclusions

This paper has introduced both an efficient method for the computation of the cuspidal configurations of a mechanism, and a reliable algorithm that partitions a given parameter space into open regions with constant number of associated cusp points.

The first one is based on a symbolic-algebraic approach able to describe the roots of exact multiplicity 3 and a certified numerical algorithm that isolates among them the real

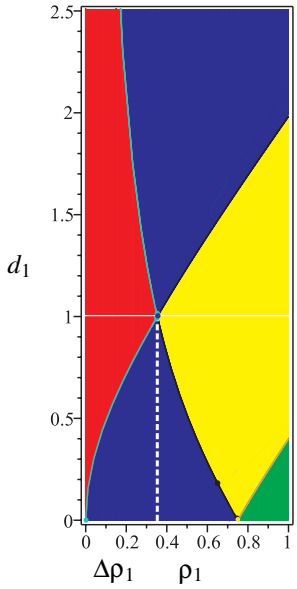

Fig. 10. Optimal d_1 and $\Delta\rho_1$ for non-cuspidal degenerate 3-RPR.

(i.e. not complex) ones. This symbolic-numeric approach is more efficient than other previously existing methods, which mainly relied on the approximation of roots of multiplicity at least 3 after reducing the initial system to a simpler one and projecting it onto the $\boldsymbol{\rho}$-space.

This new method is combined with some algebraic tools such as the discriminant variety (DV) and the cylindric algebraic decomposition (CAD) in order to analyze a 2-dimensional parameter space with respect to the associated number of cusp points. This second algorithm provides a partition of the parameter space into cells with constant number of cusp points, which is certified for whatever values are picked inside each open cell but not on their borders. Cell borders are further analyzed by Algorithm 4 based on Conjecture 1, which still remains unproved.

Both algorithms have been applied to the analysis and distribution of the cusp locus for a family of degenerate 3-RPR manipulators, and some applications to robot design are also derived. This does not mean that the two given algorithms are specially designed for this type of 3-RPR mechanisms. Indeed, they are suitable for more general examples since they do not rely on any ad-hoc formulation. Nevertheless for some examples the obtention of results within reasonable time may not be feasible yet, since there is an important symbolic-algebraic part, and thus the more complex the initial system is the harder it will be to compute a partition on the parameter space.

Acknowledgements

The authors would like to acknowledge the financial support of this research by ANR Project SiRoPa. The first and second authors have been supported for this research by two postdoctoral contracts at the Institut de Recherche en Communications et Cybernétique de Nantes under the sponsorship of the same project.

References

[1] Innocenti, C., and Parenti-Castelli, V., 1998. "Singularity-free evolution from one configuration to another in serial and fully-parallel manipulators". *ASME J. Mechanical Design,* **120**(1), pp. 73–79.

[2] McAree, P. R., and Daniel, R. W., 1999. "An explanation of never-special assembly changing motions for 3-3 parallel manipulators". *I. J. Robotic Research,* **18**(6), pp. 556–574.

[3] Zein, M., Wenger, P., and Chablat, D., 2007. "Singular curves in the joint space and cusp points of 3-RPR parallel manipulators". *Robotica,* **25**(6), pp. 717–724.

[4] Husty, M. L., 2009. "Non-singular assembly mode change in 3-RPR parallel manipulators". In Proceedings of the 5th International Workshop on Computational Kinematics, Springer, pp. 51–60.

[5] Kreuzer, M., and Robbiano, L., 2000. *Computational commutative algebra 1*. Springer.

[6] Lazard, D., and Rouillier, F., 2007. "Solving parametric polynomial systems". *J. Symbolic Computation,* **42**(6), pp. 636–667.

[7] Collins, G. E., 1975. *Quantifier Elimination for Real Closed Fields by Cylindrical Algebraic Decomposition*. Springer.

[8] Chablat, D., Moroz, G., and Wenger, P., 2011. "Uniqueness domains and non singular assembly mode changing trajectories". In Proceedings of the 2011 IEEE International Conference on Robotics and Automation (ICRA), pp. 3946–3951.

[9] Hunt, K., 1983. "Structural kinematics of in-parallel actuated robot arms". *J. Mechanisms, Transmissions and Automation in Design,* **105**, pp. 705–712.

[10] Gosselin, C., Sefrioui, J., and Richard, M., 1992. "Solutions polynomiales au problème de la cinématique directe des manipulateurs parallèles plans à trois degrés de liberté". *Mechanism and Machine Theory,* **27**(2), pp. 107–119.

[11] Pennock, G., and Kassner, D., 1990. "Kinematic analysis of a planar eight-bar linkage: application to a platform-type robot". In ASME Proc. of the 21st Biennial Mechanisms Conf., pp. 37–43.

[12] Kong, X., and Gosselin, C., 2001. "Forward displacement analysis of third-class analytic 3-RPR planar parallel manipulators". *Mechanism and Machine Theory,* **36**, pp. 1009–1018.

[13] Wenger, P., and Chablat, D., 2009. "Kinematic analysis of a class of analytic planar 3-RPR parallel manipulators". In Proceedings of the 5th International Workshop on Computational Kinematics, pp. 43–50.

[14] Wenger, P., Chablat, D., and Zein, M., 2007. "Degeneracy study of the forward kinematics of planar 3-RPR parallel manipulators". *ASME J. Mechanical Design,* **129(12)**, pp. 1265–1268.

[15] Gosselin, C., and Angeles, J., 1990. "Singularity analysis of closed-loop kinematic chains". *IEEE J. Robotics and Automation,* **6**(3), pp. 281–290.

[16] Urízar, M., Petuya, V., Altuzarra, O., and Hernández, A., 2011. "On the cuspidality of the analytic 3-RPR".

In IFToMM 13th World Congress in Mechanism and Machine Science.

[17] Hernández, A., Altuzarra, O., Petuya, V., and Macho, E., 2009. "Defining conditions for nonsingular transitions between assembly modes". *IEEE Transactions on Robotics,* **25**, pp. 1438–1447.

[18] Moroz, G., Rouillier, F., Chablat, D., and Wenger, P., 2010. "On the determination of cusp points of 3-RPR parallel manipulators". *Mechanism and Machine Theory,* **45**.

[19] Moroz, G., 2008. "Sur la décomposition réelle et algébrique des systèmes dépendant de paramètres". PhD thesis, Université Paris 6, France.

[20] Corvez, S., and Rouillier, F., 2002. "Using computer algebra tools to classify serial manipulators". In Automated Deduction in Geometry, pp. 31–43.

[21] Rouillier, F., 1999. "Solving zero-dimensional systems through the rational univariate representation". *J. Applicable Algebra in Engineering, Communication and Computing,* **9**(5), pp. 433–461.

[22] Rouillier, F., and Zimmermann, P., 2003. "Efficient isolation of polynomial real roots". *J. Computational and Applied Mathematics,* **162**(1), pp. 33–50.

[23] Dolzmann, A., Seidl, A., and Sturm, T., 2004. "Efficient projection orders for CAD". In Proceedings of the 2004 International Symposium on Symbolic and Algebraic Computation, pp. 111–118.